Establishment of a Finite Element Model of Supination-external Rotation Ankle Joint Injury and Analysis of Mechanical Changes in the Posterior Malleolar Surface

Xin Zhang
Jiading District Central Hospital Affiliated Shanghai University of Medicine &Health Sciences
Pinliang Xie
Jiading District Central Hospital Affiliated Shanghai University of Medicine &Health Sciences
Weirong Shao
Jiading District Central Hospital Affiliated Shanghai University of Medicine &Health Sciences
Ming Xu
Jiading District Central Hospital Affiliated Shanghai University of Medicine &Health Sciences
Xiaoping Xu
Jiading District Central Hospital Affiliated Shanghai University of Medicine &Health Sciences
Yong Yin (yinyong910428@126.com)
Jiading District Central Hospital Affiliated Shanghai University of Medicine &Health Sciences
Lan Fei
Jiading District Central Hospital Affiliated Shanghai University of Medicine &Health Sciences

Research Article

Keywords: Supination-external rotation, Stress distribution, Finite element analysis, Posterior malleolus

Posted Date: November 11th, 2021

DOI: https://doi.org/10.21203/rs.3.rs-1036053/v1

Abstract

Background

By establishing a three-dimensional finite element model of supination and external rotation ankle injury, the stress characteristics of the posterior ankle joint surface can be obtained, and complete analysis of the corresponding stress on the lateral ankle can be examined.

Methods

Thin-layer computed tomography (CT) images of normal ankle joints in the supination and external rotation non-weight-bearing states were selected, a three-dimensional data model of each ankle joint, including the ligament, was established, and whether different degrees of injury were coexistent with lateral ankle fracture was analysed by the finite element method. A load was applied to examine different ankle joint stress values and pressure distributions on the surface of the posterior ankle joint.

Results

When a load was applied, the maximum stress was located at the point of attachment of the anterior tibiofibular ligament to the tibia. When the anterior tibiofibular ligament was removed and the lateral malleolus was intact, the maximum stress (271.2 MPa) was located at the attachment point of the posterior tibiofibular ligament to the tibia, and the maximum pressure of the posterior ankle joint surface was 2.626 MPa. When a lateral malleolus fracture was present and the same load was applied, the maximum stress (82 MPa) was located on the fibular fracture surface, and the maximum pressure of the posterior ankle joint surface was 7.787 MPa. The posterior tibiofibular ligament was then removed completely from the lateral malleolus, and the maximum stress (132.7 MPa) was located at the point of attachment of the posterior tibiofibular ligament to the fibula, and the maximum pressure of the posterior ankle joint surface was 4.505 MPa. When a lateral malleolar fracture was present, the maximum stress (82.72 MPa) was located on the fibular fracture surface, and the maximum pressure of the posterior ankle joint surface was 8.022 MPa.

Conclusion

This study shows that reconstruction of the lateral malleolus in supination-external rotation ankle injury significantly affects the stress distribution at the posterior malleolar joint surface. When reconstruction of the lateral malleolus is complete, the pressure distribution of the posterior malleolar joint surface can be significantly reduced. The results highlight the significance of reconstruction of posterior malleolar fractures and posterior tibiofibular ligament stability.

Background

Ankle fractures account for approximately 3.9% of all systemic fractures and are a common type of intra-articular fracture. Approximately 14% to 44% of these fractures impact the posterior malleolus, and they

often result in instability of the ankle[1]. The posterior malleolus refers to the structures behind the fibular notch of the distal tibia, posterior tubercle (Volkmann tubercle), ankle sulcus and posterior colliculus of the medial malleolus. It is an integral part of the distal tibiofibular complex, increasing the contact area of the tibiotalar joint, reducing the pressure per unit area of the tibiotalar joint, preventing backward movement of the talus, and supporting and maintaining the stability of the ankle joint[2, 3]. Most posterior ankle fractures are associated with lateral ankle fractures and ligament injuries around the ankle, especially supination-external rotation ankle fractures caused by rotational violence[4]. It is rare that they appear alone; if the reduction is not good, the area is prone to traumatic arthritis, and the poor reduction affects the function of the ankle joint.

In the treatment of supination-external rotation ankle joint injury, anatomical reconstruction and rigid fixation of lateral ankle fractures are usually not difficult to carry out, but controversy exists on the type and effectiveness of fixation for posterior ankle fracture[5]. Current opinion holds that some posterior malleolar blocks, although small, have an important role in maintaining the stability of the lower tibiofibular[6]. Thus, exploring how the mechanical changes before and after external ankle reconstruction for the posterior ankle facet directly affect the stability of the posterior ankle fracture fragment and indirectly affect the lower tibiofibular and overall stability of the ankle is essential. The final results of such an analysis may suggest new ideas for the treatment of posterior ankle fractures in supination-external rotation-type injuries.

Given this, the present study simulates the integrity of the external malleolus with different degrees of injury and performs a mechanical analysis of the force situation on the surface of the posterior malleolus by establishing a finite element model of supination-external rotation ankle injury. This helps to provide a biomechanical basis for the use of complete posterior malleolar fixation in external malleolar reconstruction of supination-external rotation ankle fractures.

Materials And Methods

1 Acquisition of ankle CT images

One healthy adult volunteer with no previous history of injury, such as ankle fracture or dislocation, or pathological conditions, such as ankle arthritis, bone disease or bone tumour, was selected. The right ankle joint of the volunteer was imaged with thin-section CT, with a scanning layer thickness of 0.625 mm, resulting in 657 images of 512 × 512 pixels that were saved in the DICOM format. During the CT scan, the volunteer's ankle was non-weight-bearing in the supination position.

2 3D reconstruction and optimization

DICOM format images were imported into Mimics 21.0 software (Materialise, Belgium,), the images were segmented, and the tibia, talus, and fibula were reconstructed. Multiple bones (including the calcaneus, navicular cuneus, mediolateral cuneus, dice cuneus, and mediolateral cuneus) beneath the talus were fused to reconstruct their 3D models (Figure 1). The data extracted from the above reconstruction were

saved as .STL format files. The exported data were triangular face models that had some undesirable structural phenomena, such as deformity, distortion, and rough surfaces. The industrial software Geomagics (Studio, Geomagics; Magics, Materialise) was used to triangulate the images, reduce noise, and homogenize the data exported from Mimics 21.0, and the data were contoured to the final shape by precise surface reconstruction. Then, three-dimensional solid models were established to facilitate subsequent processing as well as finite element model building and analysis.

3 Establishment of the finite element model

The optimized 3D models were imported into SolidWorks software, and the obtained geometric models were imported into ABAQUS software (2018, Dassault, Providence, RI, USA). to build finite element models with the help of the attachment points and anatomical locations of ligaments determined from reference documentation; there was a total of 362,351 nodes and 261,420 units (Figure 1). Bone and ligaments were simplified into isotropic, homogeneous linear elastic materials, and the material parameters are listed in Table 1[7, 8]. In brief, bonding contact was used between the ligament and bone, calcaneus and talus, while the talus, tibiofibula, and intercalcaneal cartilage were in facet contact with bone. The friction coefficient was then taken as 0.2 to establish the finite element analysis model.

4 Verification and analysis of the finite element model

In this part, the model loading parameters were based on a fixed lower surface of the talus, and a dead weight loaded between the tibia and proximal fibula and the internal rotation force were used to simulate the post rotation-external rotation-type injury situation. Three directional fixation restraints were set with full degrees of freedom in XYZ at the under-surface of the talus, and a reference point was established near the upper surface of tibia and fibula, coupled with the upper surface degrees of freedom, the application of a dead weight load (480 N compression on the upper surface of the tibia and 120 N compression on the upper surface of the fibula) and the internal rotation force (gradually increased internal rotation force, simulated to an IV degree injury). A 600 N vertical compressive load was applied to the upper sections of the lower tibia and fibula of the model, the calcaneus was fixed, and the talus was constrained. The maximum contact stress of the ankle joint surface was 2.1059 MPa, the contact area was 373.658 mm^2 (Figure 2), and the model was effective[9]. The calculations of outcomes were based on the maximum stress location and pressure on the articular surface.

Results

1 Model of stage I supination-external rotation ankle injury

The maximum value of stress at 1.5 N · m internal rotation was 51.05 MPa at the attachment point of the anterior tibiofibular ligament to the fibula, and the maximum value of pressure at the posterior ankle joint surface was 2.549 MPa (Figure 3).

2 Model of stage II supination-external rotation ankle injury

When removing the anterior tibiofibular ligament, the lateral malleolus remained intact. Then, 10 N · m internal rotation was continued, and the results show that the maximum stress on the posterior tibiofibular ligament when loading the 10 N · m internal rotation force on the tibial attachment point was 271.2 MPa, and the maximum pressure at the posterior ankle joint surface was 2.626 MPa (Figure 4).

The fibula fracture line was drawn posterosuperior and inferior to construct the stage II injury fracture model (Figure 5). The calculation showed that the maximum stress on the fibula fracture surface when a 10 N · m internal rotation force was applied was 82 MPa; the maximum pressure at the posterior ankle joint surface was 7.787 MPa (Figure 6).

3 Model of stage III supination-external rotation ankle injury

With the lateral malleolus intact, a model of stage III injury was established by removing the posterior tibiofibular ligament. Loading with internal rotation was continued, and the calculated results indicated that the maximum stress after removing the posterior tibiofibular ligament was 132.7 MPa, located at the attachment point of the posterior talofibular ligament to the fibula, and the maximum pressure on the posterior ankle joint surface was 4.505 MPa (Figure 7).

On the basis of the above, fibula fracture lines were drawn from upwards and forward from the back to construct a fracture model. The calculation results showed that the maximum stress was 82.72 MPa, located at the fibula fracture surface, and the maximum value of pressure at the posterior ankle joint surface was 8.022 MPa (Figure 8).

Table 1 Material parameters

	Elastic modulus	Poisson's ratio
Name	*E* (MPa)	v
Bone	14000	0.3
Cartilage	15	0.46
Ligament	260	0.49

Discussion

Lauge-Hansen's classification, which was published in a 1950 issue of Archives of Surgery, has become one of the most widely used ankle fracture classification systems. In that article, Niel Lauge-Hansen presented an ankle fracture classification and an explanation for low-energy fractures caused by rotational violence in the ankle. This classification is based on foot position at the time of the traumatic event (supination or pronation) and the direction of the deforming forces (abduction, adduction, or external rotation). Seventy percent of these fractures were of the supination-external

rotation type: the foot was in the supination position due to external rotation violence. Stage III-IV damage involved bony structures or associated ligaments of the posterior malleolus.

Through three-dimensional heat map analysis, Yu Tao et al. found that most of the fracture lines of the posterior malleolus were concentrated in an arc-banded region that started from 1/7 to 2/7 of the tangent line of the posterior edge and ended at 5/11 to 7/11 of the tangent line of the outer edge[10]. The proportion of posterior malleolar fracture blocks to the total articular surface of the distal tibia was 14.96%[10]. In the past, a posterior malleolus fracture area of more than 25% was considered to be an indication for surgical treatment of posterior malleolar fracture. Verhage et al. found that the incidence of osteoarthritis was approximately 48% when the area of posterior malleolar fracture accounted for 5%-25% of the tibial articular surface and as high as 54% when the area was greater than 25%, and excellent reduction could not be maintained except by internal fixation[11, 12].

Mangnus et al. believed that the position of the posterior malleolar fracture line may have a greater impact on stability than the size of the fracture area; even if the posterior malleolar fracture is small, it will affect ankle joint stability[13]. Gardner et al. confirmed on postoperative CT that posterior malleolar fracture affects the stability of the inferior tibiofibular ligament, and unfixed posterior malleolar fracture can lead to tibiofibular joint subluxation[14, 15]. In recent years, after ankle fracture block fixation to restore the tibia after fibular ligament trauma and help improve tibia-fibula joint mechanics, the stability of the tibia is better than that of the tibial-fibular ligament. The purpose of the screw, so scholars think, after ankle fracture, no matter how large the fracture piece, should be anatomical reconstruction, and the number of tibia-fibula screws used should be minimized[16]. Therefore, for the treatment of posterior malleolar fractures, determining whether surgery is necessary by the size of the bone only is not reliable.

In the supination and external rotation ankle injury model constructed in this paper, the ankle joint was in the supination position when the initial CT images were collected. After the 3D model was constructed, a 600 N vertical compression load was applied to the upper section of the lower tibia and fibula of the model to fix the calcaneus and restrain the talus, which was effective for model verification. After fixation of the tibia and fibula on the lower surface of the talus, the proximal tibia and fibula were loaded with dead weight and internal rotation force to simulate supination and external rotation injury. When 1.5 N·m internal rotation force was applied, the maximum stress was located at the attachment point of the anterior tibiofibular ligament to the fibula, which was consistent with the description of the Lauge-Hansen classification in clinical practice[17].

By removing the anterior tibiofibular ligament, lateral malleolar fractures were constructed and compared with intact lateral malleolar fractures. When a 10 N·m internal rotation force was applied, the maximum stress changed from the lateral malleolar fracture to the attachment point of the posterior tibiofibular ligament to the tibia. The maximum pressure on the rear ankle joint surface decreased from 7.787 MPa to 2.626 MPa. The maximum stress position of the posterior malleolus moved significantly. By removing the posterior tibiofibular ligament, a lateral malleolar fracture was constructed, and the lateral malleolus was preserved intact. The maximum stress changed from the tibial attachment point of the tibiofibular

ligament with fracture and stage II injury to the fibula attachment point of the talar fibular ligament. In stage III injury, the maximum pressure on the posterior ankle surface decreased from 8.022 MPa to 4.505 MPa after lateral malleolar reconstruction. The stress position of the posterior malleolus did not change significantly compared with that in the stage II injury.

Based on the above data, it can be concluded that anatomic reconstruction and rigid fixation of the lateral malleolus can significantly reduce the stress of the posterior ankle surface in supination and external rotation injuries. At the same time, the completion of anatomical reconstruction will maximize the distribution of stress from the fracture end to the attachment point of the ligament, and the maximum stress site of the posterior malleolus will be significantly moved back. This means that after lateral malleolar reconstruction for supination and external rotation ankle injury is completed, the vertical instability of the posterior malleolar fracture under the action of stress will be significantly reduced, and the rotation instability due to ligament pulling will be more obvious. The maximum stress ratio is 132.7:4.5. Therefore, the establishment of rotational stability may be more important than the establishment of vertical stability for posterior ankle fractures. If the posterior ankle fracture and the stability of the posterior tibiofibular ligament are not satisfied, the maximum contact stress of the posterior ankle surface increases to more than 2 times the normal level, further aggravating ankle instability. Therefore, reconstruction of the posterior structure of the lateral malleolus in supination and external rotation ankle injuries will have an important impact on ankle stability, which is consistent with the views of Mangnus and Gardner et al[13, 14]. In terms of the choice of internal fixation method for posterior malleolar fracture, a two-screw gasket has good anti-rotation effects, while a Buttress plate causes less anti-vertical trauma. Therefore, the choice of two-screw spacers for internal fixation may be sufficient for posterior malleolar fracture in supination and external rotation ankle injury after lateral malleolar reconstruction, but further biomechanical research is needed.

Conclusion

In conclusion, this study indicates that lateral malleolar reconstruction of supination and external rotation ankle injuries is of great significance to stress distributions on the posterior ankle surface. When lateral malleolar reconstruction is completed, the pressure distribution of the posterior ankle surface can be significantly reduced, and the significance of the reconstruction of posterior malleolar fractures and the stability of the posterior tibiofibular ligament are highlighted. The deficiencies of this study have not been further explored in studies related to stage IV injury involving deltoid ligament and medial malleolar fracture, construction of posterior malleolar fractures, and selection of internal fixation methods.

Abbreviations

CT: computed tomography

Declarations

Ethics approval and consent to participate

This study was conducted in keeping with the Declaration of Helsinki and has been reviewed and approved by the ethics committee of Jiading District Central Hospital Affiliated Shanghai University of Medicine &Health Sciences, all methods were carried out in accordance with relevant guidelines and regulations. Written informed consent was obtained from the healthy adult prior to enrollment in the study as per our study protocol reviewed and approval by local institutional review boards.

Consent to publish

All authors read and approved the final manuscript.

Availability of data and materials

The datasets generated and/or analysed during the current study are not publicly available due to patient personal health confidentiality agreement but are available from the corresponding author on reasonable request.

Competing interests

The authors declared that they have no conflict of interest in this work.

Funding

The present study was supported by grants from the Foundation of Research project of health and Family Planning Commission of Jiading District, Shanghai (JDKW-2018-W15).

Authors' Contributions

XZ and PX had the study idea, wrote the proposal for the relevant committee, conducted the statistics and wrote the paper. WS and MX were responsible for data generation and participated in writing the paper, and conducted CT scans, helped prepare and analyze the data and proof-read the paper. XX participated in manuscript preparation. YY and LF were the study initiators, helped with the ethics proposal, data interpretation and proof-read the paper. All authors have read and approved the manuscript.

Acknowledgements

Not applicable.

References

1. Koval KJ, Lurie J, Zhou W, Sparks MB, Cantu RV, Sporer SM, Weinstein J: **Ankle fractures in the elderly: what you get depends on where you live and who you see**. *Journal of Orthopaedic Trauma* 2005, **19**(9):635-639.

2. Bartoníček J, Rammelt S, Kostlivý K, Vaněček V, Klika D, Trešl I: **Anatomy and classification of the posterior tibial fragment in ankle fractures**. *Archives of orthopaedic and traumatic surgery Archiv fur orthopadische und Unfall-Chirurgie* 2015, **135**(4):505-516.

3. Yasui Y, Takao M, Miyamoto W, Innami K, Matsushita T: **Anatomical reconstruction of the anterior inferior tibiofibular ligament for chronic disruption of the distal tibiofibular syndesmosis**. *Knee surgery, sports traumatology, arthroscopy : official journal of the ESSKA* 2011, **19**(4):691-695.

4. Haraguchi N, Haruyama H, Toga H, Kato F: **Pathoanatomy of posterior malleolar fractures of the ankle**. *J Bone Joint Surg Am* 2006, **88**(5):1085-1092.

5. Xiaofeng G, Yong W, Yanwei L, Yan W, Jinhui W, Manyi W: **Operative indications for posterior malleolar fractures**. *Chinese Journal of Orthopaedic Trauma* 2015, **3**(17).

6. Fu S, Zou ZY, Mei G, Jin D: **Advances and disputes of posterior malleolus fracture**. *Chin Med J (Engl)* 2013, **126**(20):3972-3977.

7. Siegler S, Block J, Schneck CD: **The mechanical characteristics of the collateral ligaments of the human ankle joint**. *Foot & ankle* 1988, **8**(5):234.

8. Chu TM, Reddy NP, Padovan J: **Three-dimensional finite element stress analysis of the polypropylene, ankle-foot orthosis: static analysis**. *Medical Engineering Physics* 1995, **17**(5):372-379.

9. Anderson D, Goldsworthy JK, Li W, Rudert MJ, Tochigi Y, Brown TD: **Physical validation of a patient-specific contact finite element model of the ankle**. *Journal of Biomechanics* 2007, **40**(8):1662-1669.

10. Tao Y, Yinqi Z, Bin L, Kai C, Hui Z, Mingzhu Z, Youguang Z, Yunfeng Y, Guangong Y: **Distribution of posterior malleolus fracture lines in ankle fracture of supination-external rotation**. *Chinese Journal of Orthopaedic Trauma* 2017, **19**(012):1015-1018.

11. Verhage, Samuel, Marinus, Hoogendoorn, Jochem, Maarten, van, Hooff, Cornelis, Christiaan: **Influence of Fragment Size and Postoperative Joint Congruency on Long-Term Outcome of Posterior Malleolar Fractures**. *Foot ankle international* 2015, **36**(6):673-678.

12. De Vries JS, Wijgman AJ, Sierevelt IN, Schaap GR: **Long-term results of ankle fractures with a posterior malleolar fragment**. *The Journal of foot and ankle surgery : official publication of the American College of Foot and Ankle Surgeons* 2005, **44**(3):211-217.

13. Mangnus L, Meijer DT, Stufkens SA, Mellema JJ, Steller EP, Kerkhoffs GM, Doornberg JN: **Posterior Malleolar Fracture Patterns**. *J Orthop Trauma* 2015, **29**(9):428-435.

14. Gardner MJ, Brodsky A, Briggs SM, Nielson JH, Lorich DG: **Fixation of posterior malleolar fractures provides greater syndesmotic stability**. *Clin Orthop Relat Res* 2006, **447**:165-171.

15. Miller AN, Carroll EA, Parker RJ, Helfet DL, Lorich DG: **Posterior malleolar stabilization of syndesmotic injuries is equivalent to screw fixation**. *Clin Orthop Relat Res* 2010, **468**(4):1129-1135.

16. Guangrong Y, Hao H: **Importance of the management of ankle fracture related problems**. *Chinese Journal of Anatomy and Clinics* 2019, **24**(2):89-92.

17. Yu Z, Chengzhi L, Yongzhong C, Jiyang Z, Cheng M, Xiuqin Q, Weidong S, Jiaming W: **Finite element modeling and mechanical analysis on supinationexternal rotation ankle injury**. *Journal of Medical Biomechanics* 2012, **27**(003):282-288.

Figures

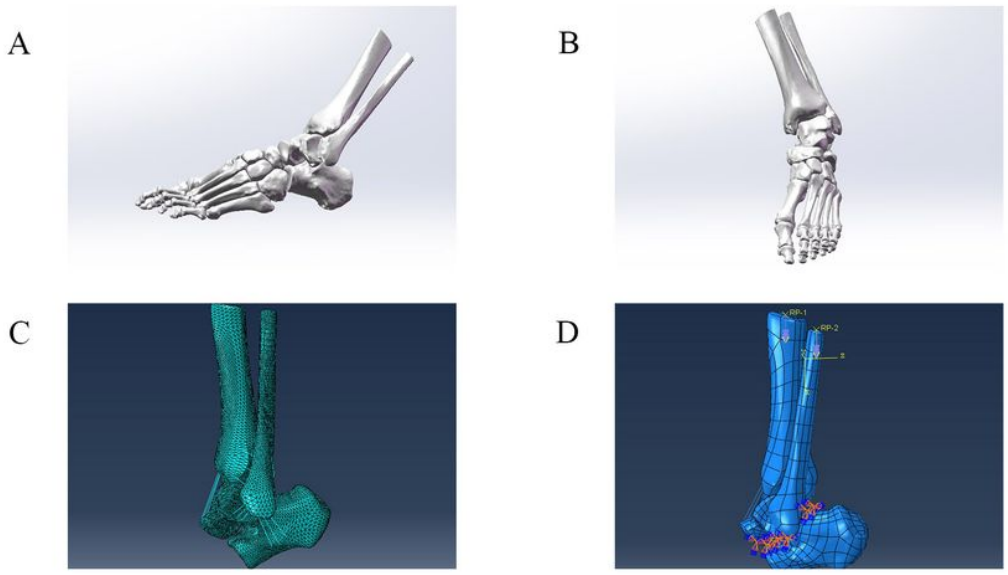

Figure 1

The process of establishing a finite element analysis model of supination-external rotation ankle injury.

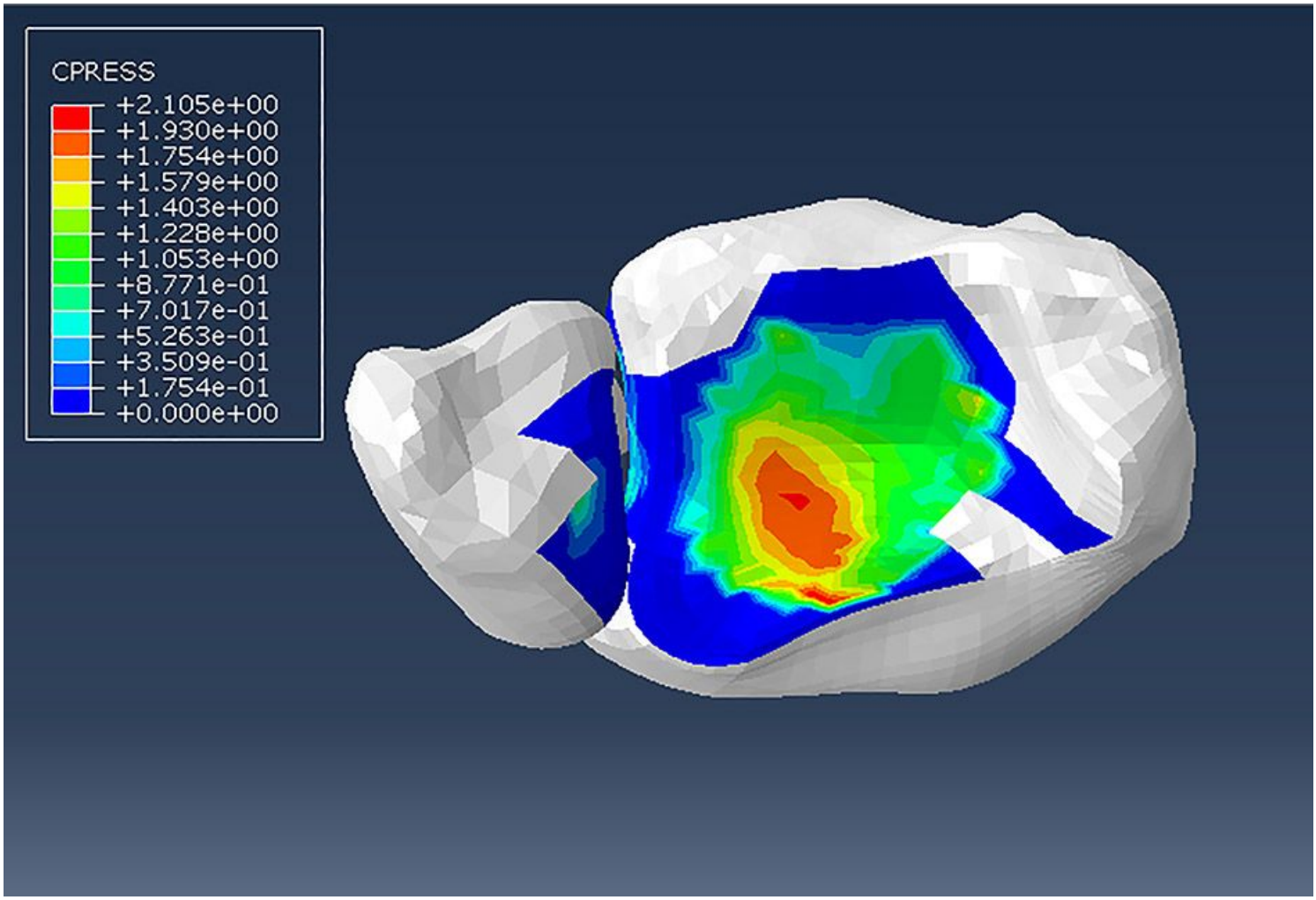

Figure 2

Validation of model validity by finite element analysis of supination-external rotation ankle injury.

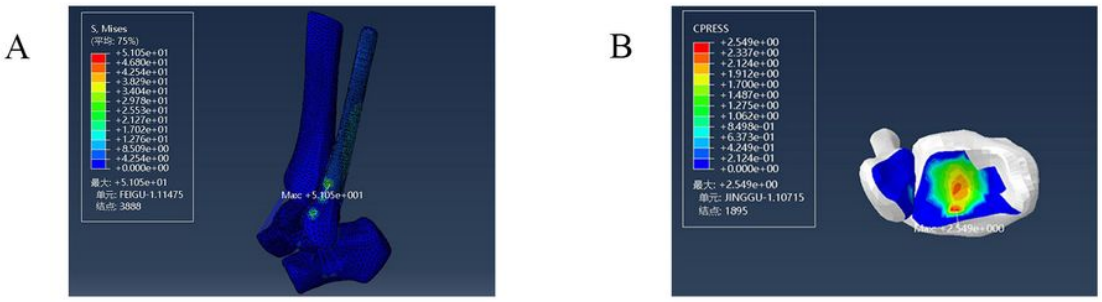

Figure 3

Stress distribution during stage I supination-external rotation ankle injury.

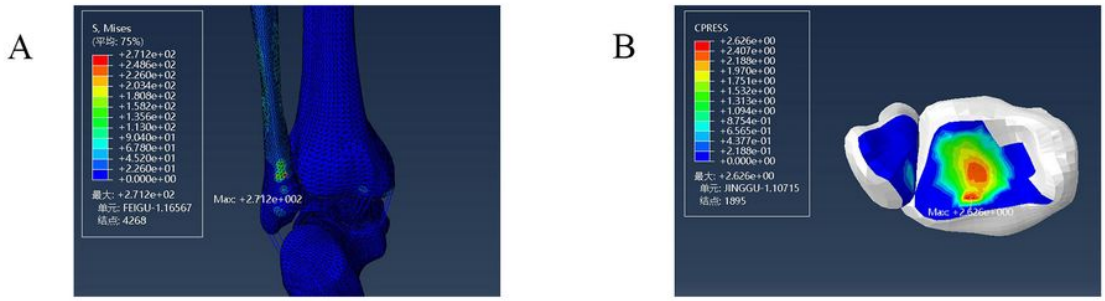

Figure 4

Distribution of stress during injury to the anterior tibiofibular ligament in supination-external rotation ankle injury.

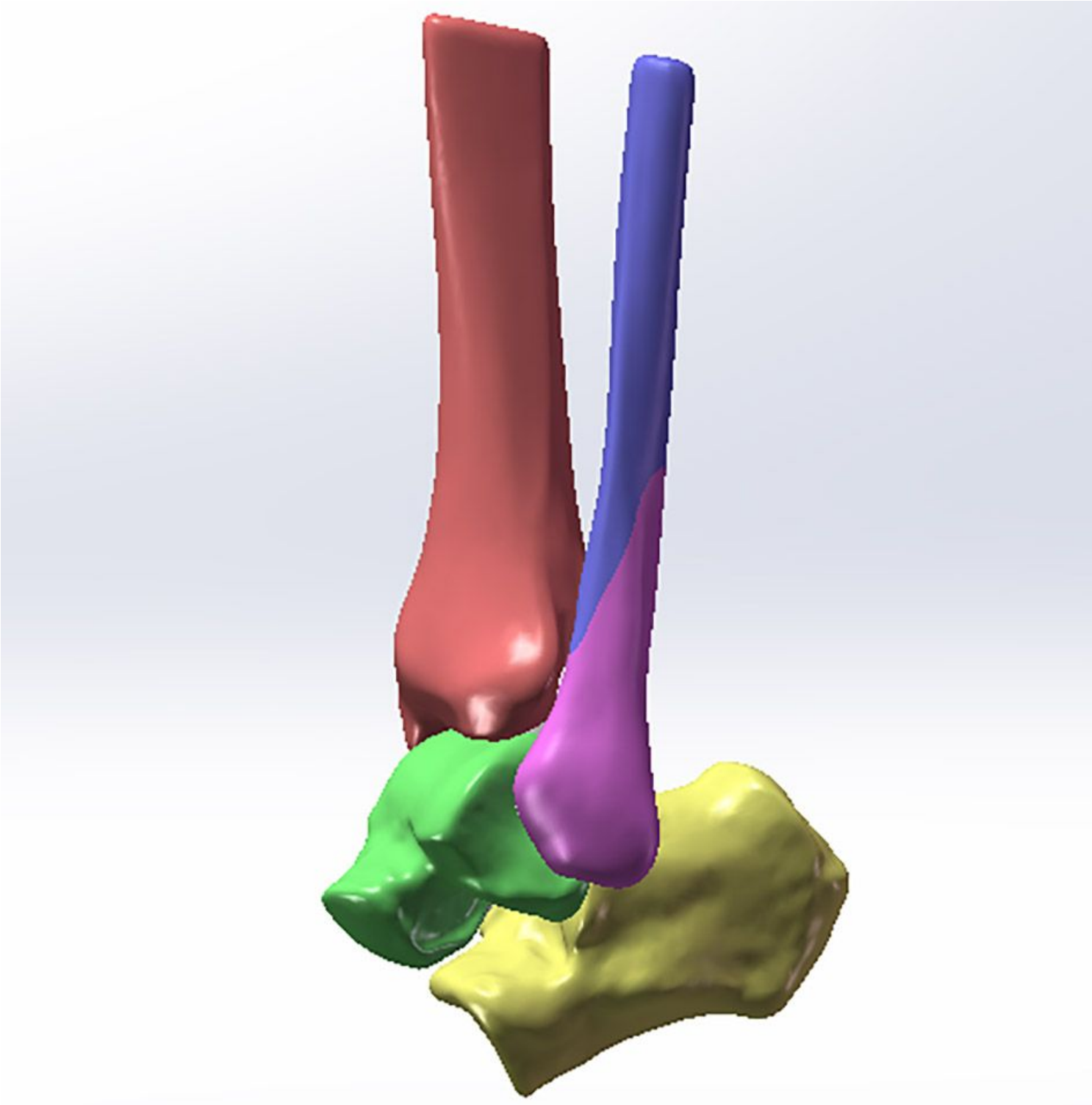

Figure 5

Model of lateral malleolar fracture in supination-external rotation ankle joint injury.

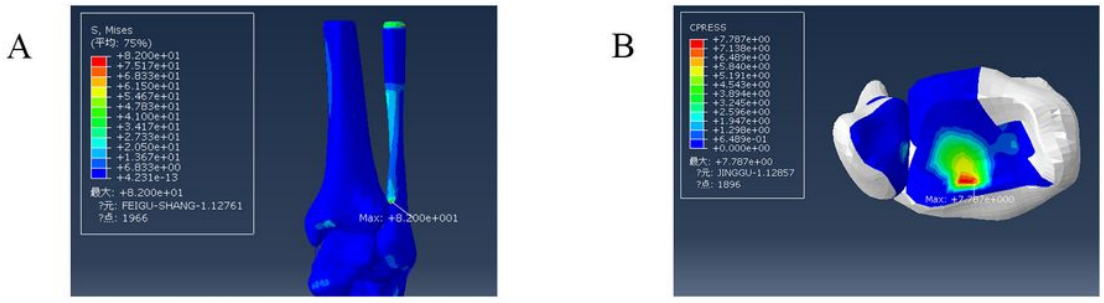

Figure 6

Distribution of stress during injury of the lateral malleolar fracture in stage II supination-external rotation ankle injury.

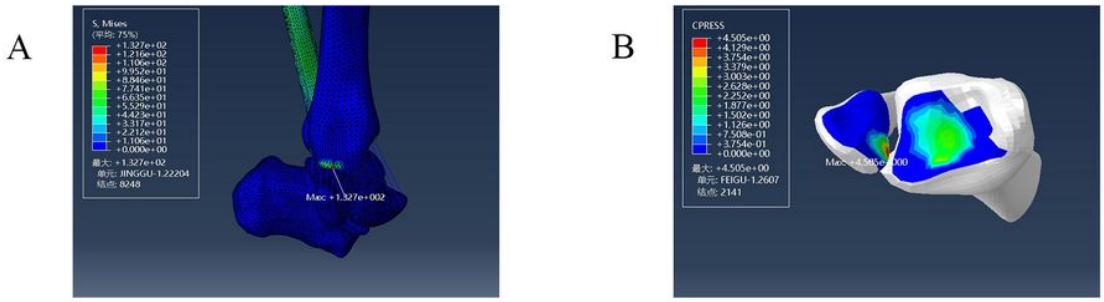

Figure 7

Distribution of stress during injury of the posterior tibiofibular ligament with stage III supination-external rotation ankle injury.

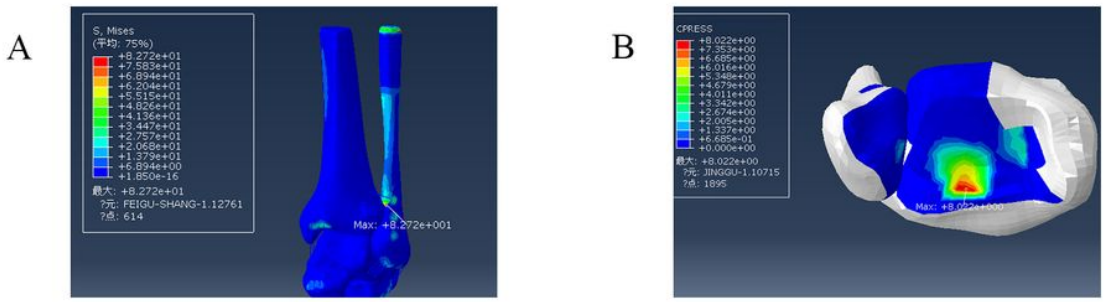

Figure 8

Stress distribution during external ankle fracture associated with injury to the posterior tibiofibular ligament with stage III supination-external rotation ankle injury.

Supplementary Files

This is a list of supplementary files associated with this preprint. Click to download.

- AJEEditingCertificate.pdf